Pressure and magnetic field dependence of valence and magnetic transitions in EuPtP

2010 J. Phys.: Condens. Matter 22 226003

(http://iopscience.iop.org/0953-8984/22/22/226003)

J. Phys.: Condens. Matter **22** (2010) 226003 (6pp) doi:10.1088/0953-8984/22/22/226003

Pressure and magnetic field dependence of valence and magnetic transitions in EuPtP

A Mitsuda[1], T Okuma[1], K Sato[2,3], K Suga[2], Y Narumi[2,4], K Kindo[2] and H Wada[1]

[1] Department of Physics, Kyushu University, 6-10-1 Hakozaki, Higashi-ku, Fukuoka 812-8581, Japan
[2] Institute for Solid State Physics, University of Tokyo, Kashiwanoha, Kashiwa 277-8581, Japan

E-mail: 3da@phys.kyushu-u.ac.jp (A Mitsuda)

Received 11 March 2010, in final form 20 April 2010
Published 12 May 2010
Online at stacks.iop.org/JPhysCM/22/226003

Abstract

The hexagonal layered compound, EuPtP, exhibits two valence transitions, at $T_1 = 235$ K and $T_2 = 190$ K, and an antiferromagnetic order at $T_N = 8.6$ K. We have examined the effects of magnetic field and pressure, and the specific heat. Analysis of the high-field experiments confirms that half of Eu are in a divalent state at the lowest temperature, and that the number of Eu^{2+} increases discontinuously at T_2 and T_1 with increasing temperature. The magnetic entropy reaches $\sim$22 J K^{-1} mol^{-1} at room temperature, which is larger than that expected for $J = 7/2$ of Eu^{2+} (17.3 J K^{-1} mol^{-1}). This is in good agreement with the magnetic entropy deduced from the interconfigurational fluctuation model, which explains the valence transition in $Eu(Pd_{1-x}Pt_x)_2Si_2$. The application of pressure shifts T_1 and T_2 higher and suppresses the intermediate phase (β phase, $T_2 < T < T_1$), whereas it does not change the properties of the low-temperature phase (γ phase, $T < T_2$) and the T_N.

(Some figures in this article are in colour only in the electronic version)

1. Introduction

A variety of exotic phenomena that arise from delocalized f electrons have been discovered and examined extensively in recent decades. A valence transition, in which the number of f electrons changes abruptly and/or significantly against temperature, pressure and magnetic field, is one such phenomenon. So far, we have focused on the valence transitions in $Eu(Pd_{1-x}Pt_x)_2Si_2$ ($0 \leqslant x \leqslant 0.15$) [1], $EuNi_2(Si_{1-x}Ge_x)_2$ ($0.5 \leqslant x \leqslant 0.82$) [2] and $Yb_{1-x}Y_xInCu_4$ ($0 \leqslant x \leqslant 0.2$) [3, 4]. These systems exhibit a Curie–Weiss paramagnetism at high temperatures. At the valence transition, the number of 4f electrons decreases in the Eu system or increases in the Yb system with decreasing temperature, accompanied by the disappearance of the localized magnetic moments and subsequent transfer into almost temperature-independent paramagnetism, such as that of Van Vleck or Pauli. These systems exhibit one valence transition into the non-magnetic phase and no magnetic order even at the lowest temperatures.

In contrast, EuPtP is a striking compound in which two first-order valence transitions, at $T_1 = 235$ K and $T_2 = 190$ K, and an antiferromagnetic order at $T_N = 8.6$ K occur [5–7]. This compound crystallizes in the hexagonal Ni_2In-type structure with one equivalent Eu site at $T > T_2$. At $T < T_2$, however, it contains two inequivalent Eu sites with a 1:1 ratio due to a slight alternate shift of a Pt–P layer [8]. At the valence transitions, the mean Eu valence shifts from a magnetic divalent ($4f^7$) state toward a non-magnetic trivalent ($4f^6$) direction with decreasing temperature. From Eu L_{III} edge x-ray absorption spectroscopy (XAS), the mean Eu valence values at $T > T_1$, $T_2 < T < T_1$ and $T < T_2$, at which the phases are called the α phase, β phase and γ phase, respectively [7], are estimated to be 2.15, 2.30 and 2.40, respectively [5]. As far as we know, EuPtP and EuNiP [7] are rare examples that exhibit two valence transitions. Below $T_N = 8.6$ K, EuPtP (γ phase) exhibits an antiferromagnetic order, which originates from stable divalent Eu ions that occupy one

[3] Present address: Department of Natural Science, Ibaraki National College of Technology, Nakane, Hitachinaka 312-8508, Japan.
[4] Present address: Institute for Materials Research, Tohoku University, Sendai 980-8577, Japan.

site of the two inequivalent Eu sites. It is considered that in the γ phase ($T < T_2$) there are layers of Eu^{2+} in one Eu site alternating in the c direction, with layers of Eu^{3+} in the other Eu site. This behavior is similar to charge order, as reported for semimetallic or semiconducting compounds such as Yb_4As_3 [9] and Eu_3S_4 [10], or to valence order, the possibility of which the authors have pointed out in a metallic YbPd system [11–13]. Unlike EuPtP, these compounds exhibit no change in the mean valence accompanied by the charge or valence order. On the other hand, in the β phase ($T_2 < T < T_1$), stacking like 223223 $\cdots$ (2: Eu^{2+} layer, 3: Eu^{3+} layer) has been speculated [7] but not yet confirmed.

In the present study, we focus mainly on the effects of magnetic field and pressure on the two valence transitions and the antiferromagnetic order. Since the Eu^{2+} ion has larger volume than the Eu^{3+} ion, it is expected that the application of pressure destabilizes the Eu^{2+} ion and shifts the Eu valence towards the trivalent direction. So far, lattice constants a and c have been measured at room temperature as a function of pressure, and high compressibility due to the valence change has been found at high pressures up to 3.0 GPa [14]. We measured the magnetization and electrical resistivity as a function of temperature under high pressures. The analysis of magnetization in pulsed magnetic fields up to 55 T and the experimental results of specific heat are also reported.

2. Experimental details

A single-crystal sample of EuPtP was grown by a Pb-flux method. Its typical shape is a rectangular parallelepiped with dimensions of 1.5 × 0.3 × 0.3 mm^3. The powder x-ray diffraction (XRD) pattern at room temperature confirms that the sample is a single phase of the hexagonal Ni_2In-type structure whose lattice constants a and c are 4.085 Å and 8.623 Å, respectively. These lattice constants are in good agreement with the previous data [5]. The SEM-EDX analysis confirms the sample composition of Eu:Pt:P = 1:1:1. Measurement of dc magnetization was carried out by a SQUID magnetometer (MPMS, Quantum Design) in the temperature range of 1.8–300 K under ambient pressure. The magnetic field was applied parallel and perpendicular to the c axis of the single-crystal sample. The magnetization of a few pieces of randomly directed single-crystal samples under pressures up to 0.64 GPa was measured in the temperature range 160–310 K by using an extraction technique. The pressure was generated by a piston–cylinder-type pressure cell made of a non-magnetic CuTi alloy. A 1:1 mixture of Fluorinert 70 and 77 was used as a pressure-transmitting medium. The pressure was determined from the pressure dependence of a Curie temperature of MnAs ($T_C \sim 317$ K under ambient pressure) [15, 16]. The high-field magnetization of the powdered sample was measured using an induction method with well-balanced pick-up coils at 4.2 K. The magnetic field, whose maximum and duration time are ∼55 T and ∼36 ms, respectively, was generated by a capacitor discharge into a non-destructive pulsed magnet made by winding coils of Cu–Ag wire. The electrical resistivity was measured by an ac four-probe method (LR-700, Linear Research) under high pressures up to 2.52 GPa in the temperature range of 2 K to room temperature. The pressure was applied by using a hybrid-type piston cylinder cell made of NiCrAl (an inner cylinder) and CuBe (an outer one) alloys and the same pressure-transmitting medium as that for the magnetization measurement. The pressure was determined from the pressure dependence of the superconducting transition temperature of Sn ($T_c \sim 3.8$ K under ambient pressure). Heat capacity was measured by means of a thermal relaxation method using the physical properties measurement system (PPMS, Quantum Design).

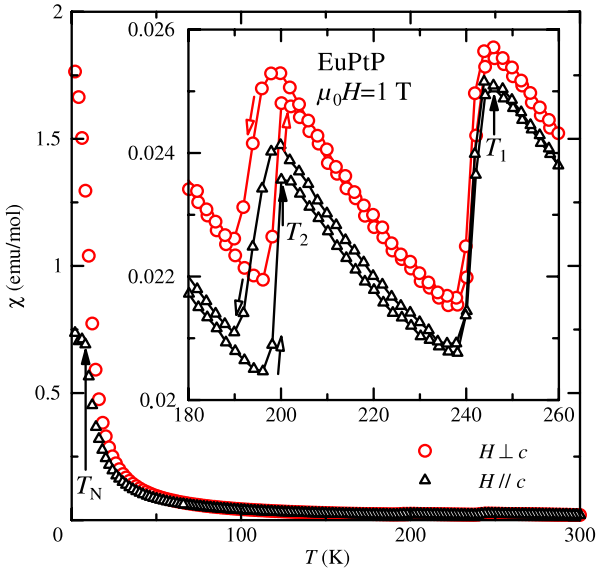

Figure 1. The magnetic susceptibility of $H \perp c$ and $H \parallel c$ is plotted as a function of temperature. The inset depicts the same data at around the valence transition temperatures, T_1 and T_2.

3. Results and discussion

Figure 1 shows the temperature dependence of magnetic susceptibility in a magnetic field of 1 T applied parallel, $\chi_\parallel$, and perpendicular, $\chi_\perp$, to the c axis. The inset of figure 1 exhibits the same data at around the valence transition temperatures. Two sharp jumps are observed with increasing temperature, which correspond to two valence transitions towards a magnetic divalent direction. The valence transition temperatures, $T_1 = 246$ K and $T_2 = 200$ K, are defined as the temperature where the χ value measured with increasing temperature has a maximum. There seems to be no difference in these valence transition temperatures between $\chi_\parallel$ and $\chi_\perp$. The thermal hysteresis is certainly found at T_2 but is hardly found at T_1, which is in qualitative agreement with the previous result [7]. The $\chi_\perp$ value is a little larger than the $\chi_\parallel$ value in the temperature range of 30–300 K. When the temperature falls below 25 K, $\chi_\perp$ increases rapidly, which is ferromagnetic behavior, while $\chi_\parallel$ increases less rapidly and there is a kink at $T = 8.1$ K in the $\chi_\parallel$–T curve, which coincides well with the antiferromagnetic order reported in [5].

Figure 2 demonstrates the magnetization process of the powdered sample in a pulsed magnetic field of 55 T at 4.2 K. The magnetization rapidly increases with increasing magnetic

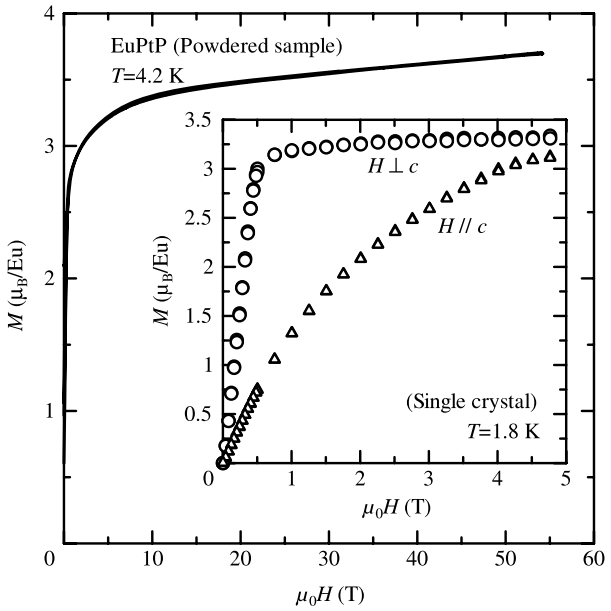

Figure 2. High-field magnetization process up to 55 T of the powdered sample at 4.2 K. The inset shows the magnetization processes of $H \perp c$ and $H \parallel c$ at 1.8 K.

field up to ∼10 T and remains close to 3.5 μ_B/Eu up to 55 T. There is no evidence of a field-induced transition. These features strongly suggest the coexistence of Eu^{2+} (7 μ_B/Eu) and Eu^{3+} (∼0 μ_B/Eu) in the ratio of 1:1, as has been pointed out in [7]. They also suggest that the rate of Eu^{2+}:Eu^{3+} = 1:1 is preserved stably even in the high magnetic field. The inset of figure 2 exhibits the magnetization processes of the single-crystalline sample in a magnetic field applied parallel and perpendicular to the c axis at 1.8 K. Magnetization perpendicular to the c axis increases rapidly and saturates to ∼3.3 μ_B/Eu. This behavior is similar to the ferromagnetic one, which coincides with the $\chi_\perp$–T curve of figure 1, but there is no spontaneous magnetization, even at 1.8 K. On the other hand, the magnetization parallel to the c axis increases mildly and tends to saturate to 3.1 μ_B/Eu at 5 T. These results mean that the magnetic easy axis is perpendicular to the c axis.

Recently, we have reported that the high magnetic field shifts T_1 and T_2 to lower temperatures [17]. Figure 3 depicts the magnetization curves at 30 K and in the temperature range of 180–300 K. Here, we analyzed these data in terms of the Brillouin function, $NgJ\mu_B B_J(x)$ ($x = g\mu_B JH/(k_B T)$) for $g = 2$ and $J = 7/2$, where N is the number of the magnetic moments of Eu^{2+}, g the Landé g-factor, J the total angular momentum, μ_B the Bohr magneton and k_B the Boltzmann factor. In this calculation, only the N value is changed as a function of temperature. Since magnetization of Eu^{3+} is sufficiently smaller than that of Eu^{2+}, we assumed that the contribution of Eu^{3+} is negligible in the present calculation. The calculated results are shown as solid circles in figure 3. At $T = 30$ K, the measured magnetization curve is roughly close to the calculated one for $N = 0.50$, which means that almost half of the Eu ions are in the divalent state. However, there is little difference between the measured and calculated curves, possibly because a molecular field was neglected. At

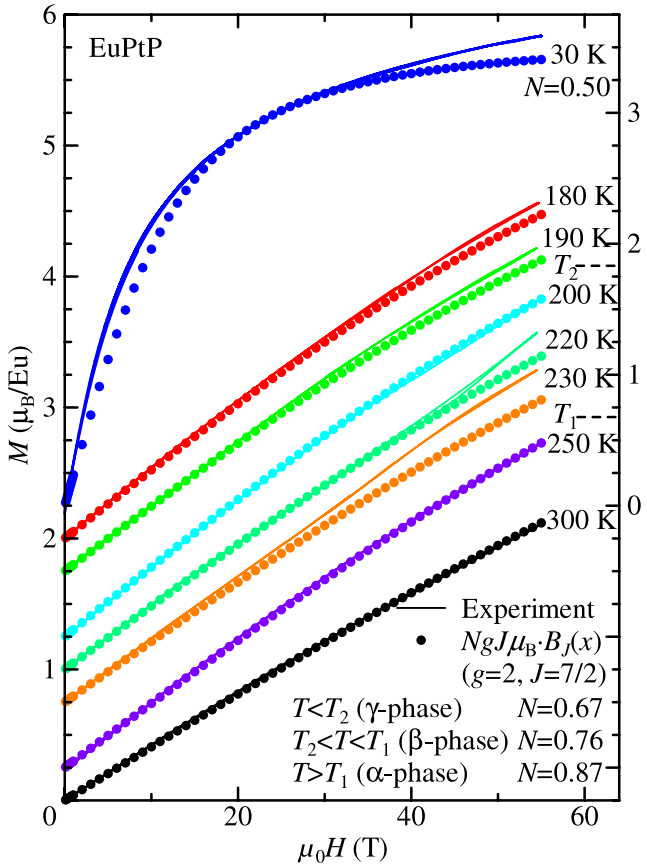

Figure 3. High-field magnetization curves up to 55 T of the powdered sample at various temperatures. Each curve is offset for clarity. Solid circles stand for $NgJ\mu_B B_J(g\mu_B JH/(k_B T))$ for $J = 7/2$.

T = 180 and 190 K (just below T_2), the measured curve almost coincides with the calculated one for $N = 0.67$, but a little deviation is observed in the high magnetic field region. The deviation field roughly corresponds to the broad maximum in the dM/dH versus H curve in [17]. Thus, the deviation reflects the field-induced valence shift associated with the valence transition at T_2. Actually, at $T = 200$ K (just above T_2), the measured curve agrees well with the calculated one for $N = 0.76$, which means the disappearance of the valence shift and a higher probability of Eu^{2+} than at $T < T_2$. At $T = 220$ and 230 K, the measured curves are in good agreement with the calculated ones in the low-field region, but again deviates remarkably upward from the calculated one in the high-field region, which corresponds to the field-induced valence shift associated with the valence transition at T_1. Above T_1, again the measured curves coincide with the calculated one for $N = 0.87$ in the whole field region. In this calculation, the N value corresponds to mean Eu valence, which is in tolerable agreement with the valence estimated from XAS. The N value also seems to decrease with decreasing temperature below T_2. This result might suggest that the Eu valence shifts toward the trivalent direction below T_2. Actually, ^{151}Eu Mössbauer spectra also change considerably: the isomeric shift of one subspectrum is towards 0 mm s^{-1} and its relative area increases with decreasing temperature [5]. This Mössbauer behavior

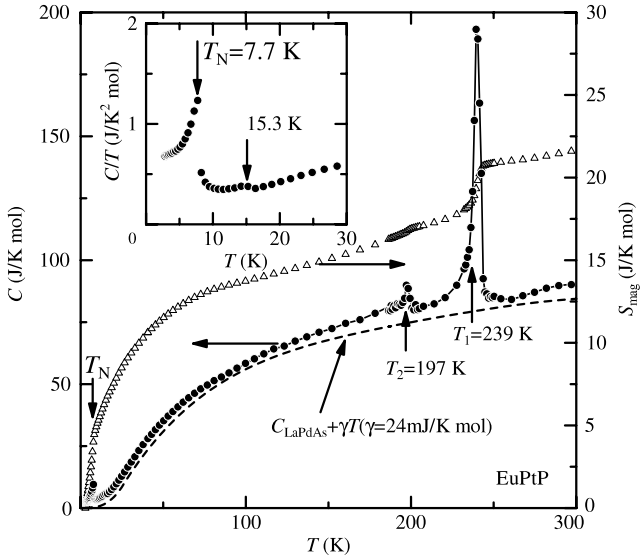

Figure 4. Heat capacity and magnetic entropy of EuPtP as a function of temperature. Three sharp peaks, corresponding to antiferromagnetic order and the valence transitions at T_1 and T_2, are observed. The inset shows the heat capacity divided by temperature versus temperature.

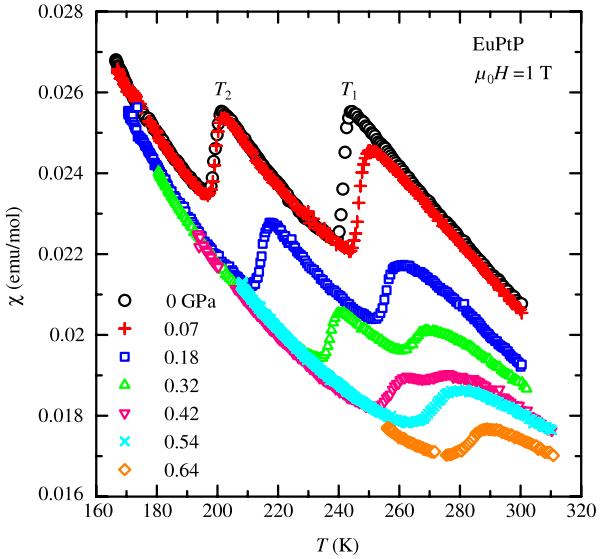

Figure 5. The magnetic susceptibility versus temperature curves under pressures up to 0.64 GPa. With increasing pressure, both T_1 and T_2 shift to higher temperature and the transitions becomes broader.

might result in the difference in the N value between 30 K and just below T_2.

To confirm the phase transitions, the specific heat, C_{EuPtP}, was measured in the temperature range of 2.5–300 K, as shown in figure 4. The inset depicts the specific heat divided by temperature as a function of temperature in the low-temperature region. One can see three obvious peaks at 7.7 K, 197 K and 239 K, which correspond to the antiferromagnetic order and the valence transitions at T_2 and T_1, respectively. The λ-like peak at 7.7 K and the sharp peak at 239.4 K suggest second-order and first-order transitions, respectively. In contrast, the peak at 197 K is much less sharp though the definite thermal hysteresis and the sharp jump at T_2 are observed in the χ–T curve (figure 1) at the same temperature. This behavior of the specific heat at T_1 and T_2 is in accordance with the previous differential thermal analysis (DTA) experiments, in which the enthalpy changes were found to be $\Delta H_1 = 0.14$ kJ mol^{-1} at T_2 and $\Delta H_1 = 0.5$ kJ mol^{-1} at T_1 [5]. At 15.3 K, a shallow anomaly is observed, which may be due to some impurity or associated with the ferromagnetism at around 25 K reported in [6]. To evaluate the magnetic entropy, S_{mag}, roughly, we attempted to subtract the specific heat for the phonon and electron contributions. However, neither contribution is easy to estimate. For the phonon contribution, because LaPtP crystallizes in the orthorhombic inverse TiNiSi-type structure, which differs from the Ni_2In-type one, the specific heat of LaTX (T = Ni, Pd, X = P, As) with the Ni_2In-type structure was compared with that of EuPtP. As a result, the specific heat of LaPdAs [19], C_{LaPdAs}, which is closer to that of EuPtP than to that of LaPdP [19] or that of LaNiP [20], was utilized as the phonon contribution. For the electron one, since the low-temperature specific heat of EuPtP contains that associated with the antiferromagnetic order at 7.7 K, as shown in the inset of figure 4, we used a Sommerfeld coefficient of $\gamma = 24$ mJ K^{-2} mol^{-1} estimated from the result of the band structure calculation for EuPdP [18], which exhibits the same structure and Eu valence state as those of γ-EuPtP. The magnetic specific heat, C_{mag}, was evaluated by subtracting $C_{\mathrm{LaPdAs}} + \gamma T$ from C_{EuPtP}. The magnetic entropy, $S_{\mathrm{mag}}(= \int (C_{\mathrm{mag}}/T)\,\mathrm{d}T)$, is demonstrated in figure 4 as a function of temperature. The S_{mag} increases definitely not only at T_N, T_2 and T_1 but also in the temperature range 10–100 K. This also suggests the gradual valence change that we have pointed out from the analysis of the high-field magnetization curve, as shown in figure 3. The magnetic entropy changes associated with T_2 and T_1 are estimated to be $\Delta S_{\mathrm{mag},2} = 0.77$ J K^{-1} mol^{-1} and $\Delta S_{\mathrm{mag},1} = 3.8$ J K^{-1} mol^{-1}, respectively. In this system, it is difficult to discuss the magnetic entropy quantitatively because it contains spin, valence and configuration contributions, which correlate with each other, and these three contributions cannot be separated. The S_{mag} saturates to ∼22 J K^{-1} mol^{-1} at around room temperature. This value is close to the calculated value (20.6 J K^{-1} mol^{-1}) in terms of the interconfigurational fluctuation (ICF) model [22], which explains the behavior of the valence transition in $Eu(Pd_{1-x}Pt_x)_2Si_2$. In this model, in addition to $J = 7/2$ for Eu^{2+}, the contribution of $J = 0$ and 1 for Eu^{3+} to magnetic entropy is taken into consideration, resulting in a larger entropy value ($\sim R \ln 12$) than the magnetic entropy of Eu^{2+} ($R \ln 8 = 17.2$ J K^{-1} mol^{-1}). The two valence transitions in EuPtP might be described in the framework of the ICM model.

To investigate the pressure effects on the two valence transitions and the antiferromagnetic order, the magnetic susceptibility and the electrical resistivity were measured under high pressure. Figure 5 indicates the temperature dependence of the magnetic susceptibility measured as the sample was heated at around T_1 and T_2 under pressures up

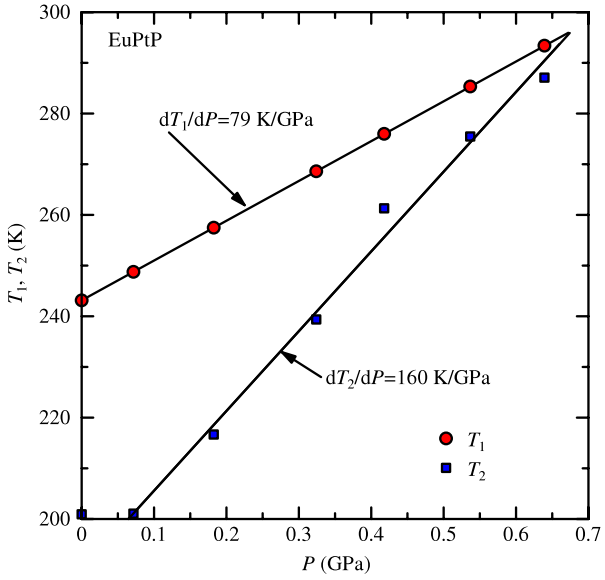

Figure 6. Pressure dependence of T_1 and T_2.

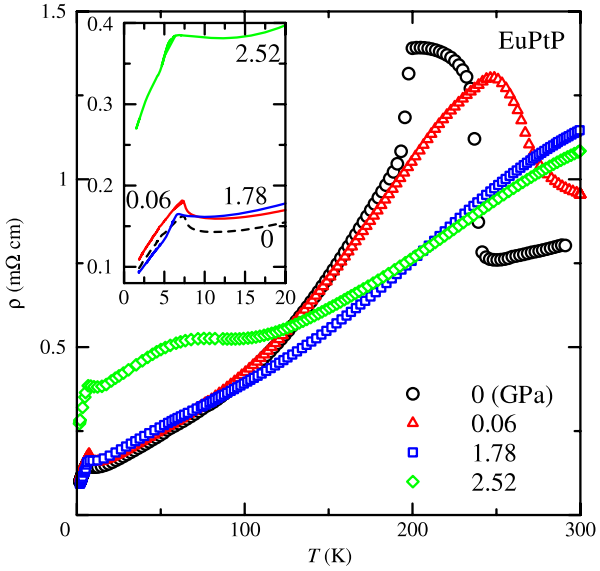

Figure 7. Electrical resistivity versus temperature curves under high pressure. The pressure values were calibrated at around 4.2 K.

to 0.64 GPa. This pressure value was determined at around room temperature. Under ambient pressure, the behavior of χ is essentially similar to that shown in figure 1. With increasing pressure, the two jumps, which correspond to the valence transitions, shift toward higher temperatures. This is reasonable behavior, since at both valence transitions, higher-temperature phases are larger in volume than lower-temperature ones. At 0.07 GPa, the T_1 shifts higher, whereas T_2 does not. This is because the pressure applied and clamped at room temperature decreases with cooling the pressure cell due to shrinkage of the pressure-transmitting medium between T_1 and T_2. With applying higher pressure, both T_1 and T_2 increase linearly with pressure, as shown in figure 6. The dT_1/dP and dT_2/dP values are estimated to be 79 K GPa^{-1} and 160 K GPa^{-1}, respectively. The large difference between dT_1/dP and dT_2/dP results in a combination of the transition at T_2 with that at T_1 and the disappearance of the β phase ($T_2 < T < T_1$). With increasing pressure, both transitions becomes broader, which implies that the transitions transfer into a second-order one. These features coincide well with the previous description of Eu(Pt$_{1-x}$Pd$_x$)P [7], assuming that the substitution of Pd for Pt corresponds to the hydrostatic pressure. This assumption is reasonable because Pd and Pt atoms belong to the same family in the periodic table and a Pd atom is smaller than a Pt one. The χ values at $T < T_2$ under various pressures seem to lie on a common curve, which means the properties of the γ-EuPtP are insensitive to pressure. On the other hand, that at $T > T_1$ is being suppressed considerably with increasing pressure, which suggests that the Eu valence of the α-EuPtP is changed considerably towards a trivalent direction. Actually, the high compressibility in the c direction was reported at room temperature for EuPtP below 2.5 GPa [14]. Since the transitions at T_1 and T_2 are of first order, the Clausius–Clapeyron (CC) relation, $dT/dP = \Delta V/\Delta S$, is applicable to these transitions. According to the results reported in [5], volume changes of ΔV_1 at T_1 and ΔV_2 at T_2 are 5.1×10^{-7} m^3 mol^{-1} and 3.9×10^{-7} m^3 mol^{-1}, respectively. The magnetic entropy changes of $\Delta S_{\mathrm{mag},1}$ at T_1 and $\Delta S_{\mathrm{mag},2}$ at T_2 are estimated to be 3.8 J K^{-1} mol^{-1} and 0.77 J K^{-1} mol^{-1}, respectively, from the present result of the specific heat. From these data, the values of $\Delta V/\Delta S$ are calculated to be $\Delta V_1/\Delta S_{\mathrm{mag},1} = 134$ K GPa^{-1} and $\Delta V_2/\Delta S_{\mathrm{mag},2} = 500$ K GPa^{-1}, both of which are in the same order as the respective experimental dT/dP values. The CC relation could not explain the dT/dP value quantitatively, but reproduces the relation of $dT_1/dP < dT_2/dP$.

Figure 7 shows the electrical resistivity as a function of temperature under high pressure up to 2.52 GPa. This pressure, which was calibrated at around 4.2 K, is ∼0.2–0.3 GPa lower than that calibrated at room temperature. At ambient pressure, a sharp jump at T_2 and a drastic drop at T_1 are observed, which is in good agreement with the previous result [21]. At 0.06 GPa, which probably corresponds to 0.32 GPa in figure 5, both transitions at T_1 and T_2 shift toward higher temperature and become much broader. At 1.78 and 2.52 GPa, both transitions possibly shift to higher temperatures than 300 K. The tendency toward saturation of the ρ at 1.78 GPa is observed at around 300 K, which possibly suggests the valence transition at T_2. The inset of figure 7 depicts the same data at temperatures below 20 K. At 7.3 K, a small peak, which is associated with the antiferromagnetic order, is observed at 0 and 0.06 GPa. Above 1.78 GPa, the peak, which becomes smaller, shifts slightly to a lower temperature. This means the antiferromagnetic order is stable in contrast to the behavior of T_1 and T_2. Taking into consideration the high-field magnetization process (figure 2) and the magnetic susceptibility under pressures (figure 5), the γ phase is quite insensitive to magnetic field and pressure. However, the slight shift of T_N to lower temperature implies that much higher pressure might collapse the antiferromagnetic order and give rise to more trivalent Eu ions, which are observed at $T < 90$ K in EuNiP [7]. Actually, at 2.52 GPa, a new broad hump

is found at around 70 K. This mechanism is unknown but reminds us of the Kondo effect or the valence fluctuation, which destabilizes the localized magnetic moment. Thus, higher-pressure experiments are desired.

4. Conclusion

We have reported on the effects of magnetic field and pressure on the valence transitions at T_1 and T_2 and the antiferromagnetic order at T_N. Analysis of the high-field magnetization measurement confirms that half of the Eu are in a divalent state at the lowest temperature, and that the number of Eu^{2+} increases at T_2 and T_1 discontinuously with increasing temperature. The application of pressure shifts the T_1 and T_2 higher and suppresses the β phase ($T_2 < T < T_1$), whereas it does not change the properties of the γ phase ($T < T_2$) or the T_N. That is, the α and β phases are sensitive to pressure, while the γ phase is insensitive. The magnetic entropy reaches $\sim$22 J K^{-1} mol^{-1} at room temperature, which is larger than that expected for $J = 7/2$ of Eu^{2+} (17.3 J K^{-1} mol^{-1}). This is close to that calculated from the ICF model.

Acknowledgment

The authors thank Dr M Watanabe at the Center of Advanced Instrumental Analysis, Kyushu University for helping us perform the SEM-EDX analysis.

References

[1] Mitsuda A, Wada A, Shiga M, Katori H A and Goto T 1997 *Phys. Rev.* B **55** 12474
[2] Wada H, Nakamura A, Mitsuda A, Shiga M, Tanaka T, Mitamura H and Goto T 1997 *J. Phys.: Condens. Matter* **9** 7913
[3] Zhang W, Sato N, Yoshimura K, Mitsuda A, Goto T and Kosuge K 2002 *Phys. Rev.* B **66** 024112
[4] Mitsuda A, Goto T, Yoshimura K, Zheng W, Sato N, Kosuge K and Wada H 2002 *Phys. Rev. Lett.* **88** 137204
[5] Lossau N, Kierspel H, Langen J, Schlabitz W, Wohlleben D, Mewis A and Sauer Chr 1989 *Z. Phys.* B **74** 227
[6] Lossau N, Kierspel H, Michels G, Oster F, Schlabitz W, Wohlleben D, Sauer Chr and Mewis A 1989 *Z. Phys.* B **77** 393
[7] Michels G, Huhnt C, Scharbrodt W, Schlabitz W, Holland-Moritz E, Abd-Elmeguid M M, Micklitz H, Johrendt D, Keimes V and Mewis A 1995 *Z. Phys.* B **98** 75
[8] Lux C, Mewis A, Lossau N, Michels G and Schlabitz W 1991 *Z. Anorg. Allg. Chem.* **593** 169
[9] Ochiai A, Li D X, Haga Y, Nakamura O and Suzuki T 1993 *Physica* B **186–188** 437
[10] Pott R, Guntherodt G, Wichelhaus W, Ohl M and Bach H 1982 *Valence Instabilities* (Amsterdam: North-Holland) p 565
[11] Pott R, Boksch W, Leson G, Politt B, Schmidt H, Freimuth A, Keulerz K, Langen J, Neumann G, Oster F, Röhler J, Walter U, Weidner P and Wohlleben D 1985 *Phys. Rev. Lett.* **54** 481
[12] Mitsuda A, Yamada K, Sugishima M and Wada H 2009 *Physica* B **404** 3002
[13] Sugishima M 2010 *J. Phys. Soc. Japan* submitted
[14] Huhnt C, Michels G, Schlabiz W, Johrendt D and Mewis A 1997 *J. Phys.: Condens. Matter* **9** 9953
[15] Menyuk N, Kafalas J A, Dwight K and Goodenough J B 1969 *Phys. Rev.* **177** 942
[16] Edwards L R and Bartel L C 1972 *Phys. Rev.* B **5** 1064
[17] Mitsuda A, Okuma T, Wada H, Sato K and Kindo K 2010 *J. Phys.: Conf. Ser.* **200** 012119
[18] Felser C, Cramm S, Johrendt D, Mewis A, Jepsen O, Hohlneicher G, Eberhardt W and Andersen O K 1997 *Europhys. Lett.* **40** 85
[19] Kato K, Terui G, Niide Y, Oyamada A and Ochiai A 2002 *J. Alloys Compounds* **339** 236
[20] Kosaka M 2009 private communication
[21] Nowack A, Klug J, Lossau N and Mewis A 1989 *Z. Phys.* B **77** 381
[22] Wada H, Gomi H, Mitsuda A and Shiga M 2001 *Solid State Commun.* **117** 703